Magnitude-frequency analysis of bed load data in an Alpine boulder bed stream

M. A. Lenzi, L. Mao, and F. Comiti

Department of Land and Agroforest Environments, University of Padua, Padua, Italy

Received 17 December 2003; revised 19 April 2004; accepted 3 May 2004; published 7 July 2004.

[1] The purpose of this study is to investigate the connection between bed load, channel processes, and sediment sources in mountain basins using data from the Rio Cordon basin (northeastern Italian Alps). The main channel is a steep, boulder bed, step pool stream, and bed load volumes are measured at a special facility where particles >20 mm are trapped. Results from a combined frequency analysis of peak water discharges and total bed load volumes based on 17 years of field data are presented, focusing on discrepancies between recurrence intervals of peak discharge and bed load volume for each event. A cause of major disturbance is a high-magnitude, low-recurrence event that occurred in 1994. Dimensional and nondimensional bed load intensity-duration curves are also reported, which emphasize differences between short- and long-duration events. The relationship flow–bed load rates (investigated using a total of 180 data) shows no breakpoints, and two different curves are evident, representing pre-1994 and post-1994 floods, respectively. The analysis demonstrates both the control exerted by sediment availability on bed load transport rates and the persisting long-term impact of major floods on mountain streams. *INDEX TERMS:* 1815 Hydrology: Erosion and sedimentation; 1821 Hydrology: Floods; 1860 Hydrology: Runoff and streamflow; 1824 Hydrology: Geomorphology (1625); *KEYWORDS:* bed load, steep channels, sediment supply, frequency analysis, step pool, Alpine torrents

Citation: Lenzi, M. A., L. Mao, and F. Comiti (2004), Magnitude-frequency analysis of bed load data in an Alpine boulder bed stream, *Water Resour. Res.*, *40*, W07201, doi:10.1029/2003WR002961.

1. Introduction

[2] In mountain basins, bed load volumes represent the primary source of concern, more than flood water volumes. Many investigations have been carried out both analytically and in the laboratory to find reliable bed load transport equations. However, very few [*Meyer-Peter and Muller*, 1948; *Mizuyama*, 1977; *Smart and Jaeggi*, 1983; *Smart*, 1984; *Bathurst et al.*, 1987; *Rickenmann*, 1990; *Suszka*, 1991] have been developed for steep boulder bed channels, where roughness conditions, sediment grading, and hydraulic phenomena make these streams completely different from lower-gradient gravel or sand bed ones.

[3] Furthermore, research aiming at validating these bed load formulae with field data has been rather scarce [*Johnejack and Megahan*, 1991; *Blizard*, 1994; *Rickenmann*, 1994, 1997, 2001; *Asti*, 1999; *D'Agostino and Lenzi*, 1999] because of the obvious problems of measuring very coarse sediment transport occurring only at very high flow rates. Frequency of bed load movement can be idealized to be a function of the ratio hydraulic driving force over channel resisting forces, and poorly sorted mountain rivers may require extremely high, infrequently occurring discharges for the mobilization of the coarsest clast size, so that annually, only a portion of finer (gravel and cobble) particles is likely to be entrained [*Knighton*, 1998; *Wohl*, 2000].

[4] Bed load transport in coarse-grained streams has been described [*Jackson and Beschta*, 1982; *Carling*, 1988] to occur in phases, with low rates (phase 1) until a certain flow stage which corresponds to a threshold above which a substantial bed load rate increase appears, this being accompanied also by a similar increase in the size of the mobilized sediment (phase 2). The beginning of phase 2 is reckoned to occur at or near the bank-full stage [*Parker et al.*, 1982; *Andrews*, 1984; *Andrews and Nankervis*, 1995], but the threshold may be poorly defined [*Ryan et al.*, 2002]. In fact, the discharge needed to start phase 2 is presumably affected by several factors, the same involved in the initiation of particle motion, such as relative roughness, clustering of individual grains, geometry of bed particles, imbrication, and packing of surface grains [*Ryan et al.*, 2002]. However, even if bed load rate can reach very high values during phase 2, its duration is relatively short over the year, especially in boulder bed streams, so that a substantial amount of the total sediment load may be due to phase 1 transport [*Andrews and Smith*, 1992; *Wilcock and McArdell*, 1993; *Lisle*, 1995]. A more complex classification of bed load transport has also been proposed [*Ashworth and Ferguson*, 1989] with phase 1 consisting of overpassing sand, phase 2 occurring at moderate flows when size-selective entrainment takes place, and finally phase 3 at the highest discharges with equal-mobility conditions. *Warburton* [1992] actually identified in the field three similar bed load phases in a proglacial step pool stream.

[5] Hillslope and tributary processes such as landslides and debris flows may deliver practically unlimited sediment supply to medium-intensity, more frequent flood events that otherwise would transport only small amounts of sediment. The degree of coupling between channel and hillslope

0043-1397/04/2003WR002961$09.00

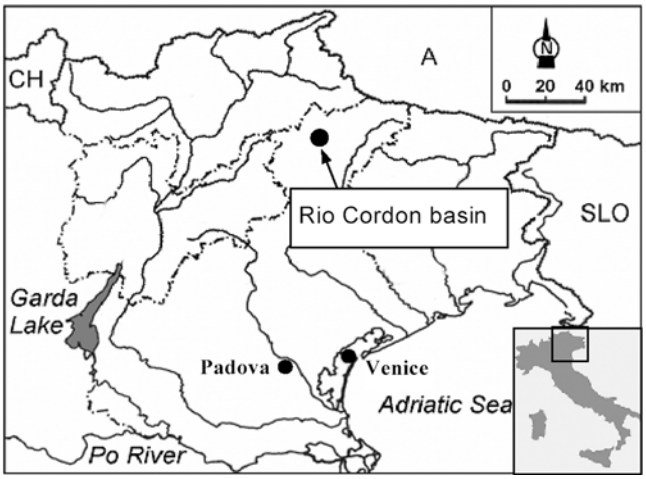

Figure 1. Rio Cordon location.

processes is a key issue in mountain basins because its variation over the years imparts large interannual differences in bed load yield as a result of changes in sediment supply to the channel. *Bogen* [1995] effectively depicts mountain rivers as a number of local erosion and sedimentation subsystems and therefore records of sediment yield may not characterize the system as a whole. As pointed out by *Wohl* [2000], in the absence of widely applicable and reliable predictive equations for bed load yield, its assessment can be extrapolated from available records of sediment yields, thus stressing the relevance of measuring facilities providing temporal series of bed load data.

[6] The aim of this study is to present and to examine 17 years of flow and bed load records measured directly at the facility in the Rio Cordon basin (Dolomites, Italian Alps), which have provided 21 flood events that have been analyzed statistically in order to estimate return intervals of both water peak discharge and bed load total and partial volumes. The occurrence of two different instances of "unlimited" sediment supply during the recorded period will also allow us to analyze their effect on bed load yield of the catchment. Finally, the relationship between water discharge and bed load rate will be analyzed, given the availability of 180 hourly bed load transport rates.

2. Materials and Methods

2.1. Study Basins and Measuring Station

[7] The research was conducted in the Rio Cordon catchment (Figure 1), a small water course of the Dolomites (eastern Italian Alps). The main physiographic characteristics of the instrumented watershed are reported in Table 1.

[8] The Rio Cordon is a steep, cobble/boulder bed channel with a prevalent step pool morphology draining a small (5 km^2) high-altitude catchment where snow-related processes (i.e., snowpack accumulation and snowmelt runoff) dominate from November to May. However, the response time of such a small basin is very short; thus important flood events occur during intense, short-duration rainfall. Flood duration is accordingly brief, so that the flow is capable of transporting sediment down the channel during only a limited time period (i.e., few hours per year), given the coarseness of the stream bed material. On average, only one to two events per year are able to cause bed load transport in the Rio Cordon.

[9] The solid geology consists of dolomites, which make up the highest relief in the catchment area, volcaniclastic conglomerates and tuff sandstones (Wengen group). In the lower part of the watershed the Buchenstein group consists of calcareous, calcareous-marly, and arenaceous rock outcrops. Quaternary moraine and scree deposits are also very common. Soils are generally thin and belong to three main families: (1) skeletal soils, occurring on steep slopes with a discontinuous vegetation cover; (2) organic soils, with more continuous and dense vegetation cover than the previous group; and (3) brown earth soils. Climatic conditions are typical of Alpine environments. Precipitation occurs mainly as snowfall from November to April. Runoff is usually dominated by snowmelt in May and June, but summer and early autumn floods represent an important contribution to the flow regime. Usually, late autumn, winter, and early spring lack noticeable runoff.

[10] The main channel features are cascade and step pool reaches, as defined by *Montgomery and Buffington* [1997]. Its average bed surface grain size distribution is characterized by the following percentiles (in mm): $D_{16} = 20$, $D_{50} = 90$, $D_{84} = 260$, and $D_{90} = 330$ [*Lenzi et al.*, 1999]. The mean diameter D_m is 130 mm. Channel width at flood flows varies in a typical cross section just upstream of the station from 4.8 to 7.6 m depending on discharge.

[11] Facilities for monitoring water discharge, suspended sediment, and bed load transport at the Rio Cordon experimental station have been described in detail previously [*Fattorelli et al.*, 1988; *Lenzi et al.*, 1999]. Measurements are taken by separating coarse grains (minimum size of 20 mm in diameter) from water and fine sediment. The measuring station consists of an inlet flume, an inclined grid where the separation of coarse particles takes place, a storage area for coarse-sediment deposition, and an outlet flume to return water and fine sediment to the stream (Figure 2). The volume of bed load is measured at 5 min intervals by 24 ultrasonic sensors fitted on a fixed frame over the storage area [*Lenzi et al.*, 1999]. Suspended sediment is measured by two turbidimeters: a Partech SDM-10 light absorption and a Hach SS6 light-scatter instrument. Flow samples are gathered automatically using

Table 1. Main Characteristics of the Rio Cordon Basin and Channel

Parameter	Value
Basin area, km^2	5.00
Average elevation, m above sea level	2200
Minimum elevation, m above sea level	1763
Maximum elevation, m above sea level	2748
Mean hillslope gradient, %	52
Length of the main channel (from the divide to the station), km	2.84
Mean width of the main channel, m	5.7
Mean gradient of the main channel (from the divide to the station), %	17
Mean gradient of the channel upstream of the station (1 km), %	13.6
Annual precipitation, mm	1100
Maximum water discharge measured, $m^3\ s^{-1}$	10.4
Mean water discharge measured, $m^3\ s^{-1}$	0.26
Minimum water discharge measured, $m^3\ s^{-1}$	0.05

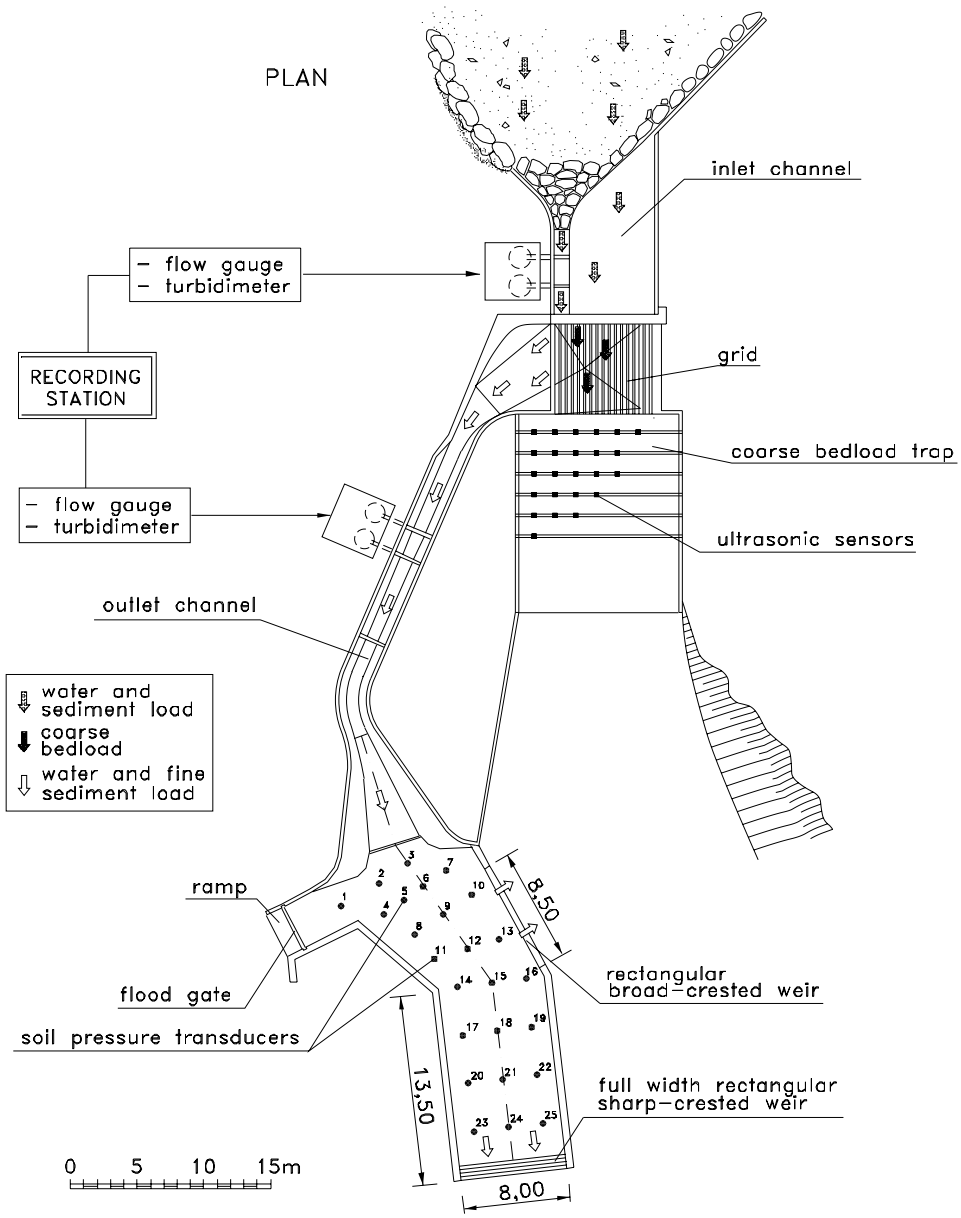

Figure 2. Plan of the Rio Cordon recording station.

a Sigma pumping sampler installed at a fixed position in the inlet channel.

[12] Sediments in the Rio Cordon basin are supplied from a number of distinctive source areas (Figure 3) which have been mapped and monitored since 1987 by field surveys and cover a total area of 0.262 km^2 (i.e., 5.2% of basin area). For each area, sketches, photographs, and sediment samples were taken [*Billi et al.*, 1998]. Their particle size distributions showed that the material of active sediment sources is widely variable from silt to gravel. Active sediment sources are mainly bare slopes, overgrazed areas, shallow landslides, eroded stream banks, and minor debris flow channels. In the Rio Cordon basin the rocky slopes commonly do not directly supply sediment to the stream channel. At most sites, sediment eroded from rock cliffs is temporarily stored as scree deposits on talus slopes. About 50% of the total sediment sources area is located upstream of a median, low-gradient belt where conditions favorable to deposition prevail. For this reason, the basin headwaters, regardless of the local intensity of the erosion processes, provide a minor contribution to the sediment yield [*Dalla Fontana and Marchi*, 2003].

[13] Previous studies in Rio Cordon have focused on bed load data [*D'Agostino et al.*, 1994; *Rickenmann et al.*, 1998; *Asti*, 1999; *D'Agostino and Lenzi*, 1999; *Lenzi et al.*, 1999], morphological structure and sedimentology of the stream bed [*Lenzi*, 2001], analysis of sediment sources [*Dalla Fontana and Marchi*, 1998, 2003], and particle transport distances [*Lenzi*, 2004]. Finally, suspended sediment concentrations and yields from single flood events have also been analyzed [*Asti*, 1999; *Lenzi and Marchi*, 2000; *Lenzi et al.*, 2003].

2.2. Data Acquisition and Validation

[14] The facility for measuring coarse sediment transport (here assumed to represent bed load) is provided with

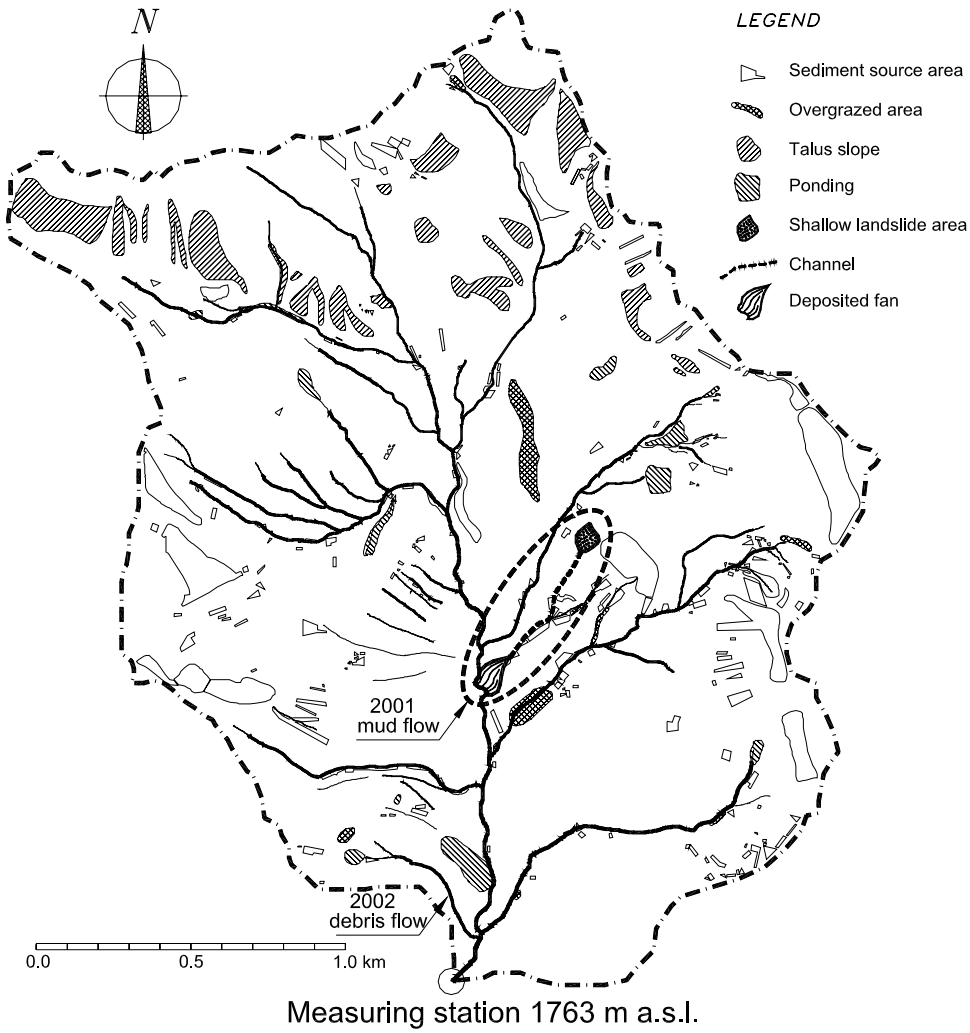

Figure 3. Map of the Rio Cordon basin showing sediment source areas. 2001 mud flow and 2002 debris flow locations are marked as well.

24 ultrasonic sensors that allow recording of the volume of the accumulation at 5 min intervals. Given the pulsating character of bed load transport and the settling of clasts forming the sediment heap, the hourly increase of bed load volume was evaluated and will represent the shortest duration analyzed hereafter. However, registration at 5 min intervals served to determine the critical discharges for bed load initiation (Q_{cr1}) and finish (Q_{cr2}), which are needed to calculate the effective runoff for each event (i.e., the hydrograph volume above the threshold of motion). Liquid discharge is also continuously measured at 5 min interval by three different flow gauges in the measuring station (Figure 2). In order to correlate an hourly bed load transport with a single liquid discharge each bed load partial volume (i.e., the increase in volume detected by the ultrasonic sensors) was associated to the previous flow rates, therefore coupling hourly bed load intensities with water discharges averaged over the antecedent 60 min throughout each flood event.

[15] From 1987 to 2003 (17 years), 21 floods characterized by bed load transport (grain size >20 mm) have been recorded at the measuring station. Hydrological and sediment load data for the flood events are shown in Table 2. It is important to bear in mind that hereafter, if not otherwise explicitly stated, bed load volumes includes the porosity of accumulation (i.e., bulk measure), estimated as 0.37 [*D'Agostino and Lenzi*, 1999].

[16] Hourly bed load transport rates are available for all the events except June 1991, October 1996, and May 2001, for which only final bed load volumes are available. For the July 1988, May 1990, June 1997, and May 2003 floods, because of the very small dimensions of the transported volumes, the ultrasonic sensors could not be activated, and final volumes were evaluated by field survey. Also, for these four flood events, critical discharges are not available; therefore they are not considered in the analysis of the effective runoff (section 6).

3. Frequency Analysis of Flood Events: Peak Discharge and Total Bed Load Volume

[17] In order to evaluate their frequency of occurrence the return interval of each flood was estimated from values of annual maximum instantaneous water discharge over 17 years (Figure 4a), i.e., selecting for each year the largest event in the case of multiple floods per year. Using the software STATISTICA 6.1 [*StatSoft*, 2002], the

Table 2. Main Hydrological and Hydraulic Features of the Major Recorded Floods[a]

	Q_p, m^3 s^{-1}	RI_{Qp}, years	BL, m^3	RI_{BL}, years	Q_{cr1}, m^3 s^{-1}	Q_{cr2}, m^3 s^{-1}	T_{BL}, hours	R_e, 10^3 m^3	BL_R, m^3 h^{-1}
11 Oct. 1987	5.2	5.6	54.8	3.2	1.8	3.8	8.0	79.9	6.9
15 July 1988	2.4	1.6	1.0	1.1	-	-	-	-	-
3 July 1989	4.4	3.9	85.0	4.1	2.2	2.7	27.0	103.4	3.1
22 May 1990	0.9	1.0	1.0	1.1	-	-	-	-	-
17 June 1991	4.0	3.3	39.0	2.7	2.00	2.40	20.0	57.9	2.0
5 Oct. 1992	2.9	2.0	9.3	1.6	1.9	2.1	10.0	21.5	0.9
2 Oct. 1993	4.3	3.7	13.7	1.7	2.30	3.70	6.0	30.7	2.3
18 May 1994	1.8	1.2	1.0	1.1	1.6	1.6	12.0	5.4	0.1
14 Sept. 1994	10.4	52.6	900.0	30.0	1.8	3.3	4.0	26.6	225.0
13 Aug. 1995	2.7	1.8	6.2	1.4	1.8	2.0	1.0	1.8	6.2
16 Oct. 1996	3.0	2.0	57.0	3.3	1.8	2.0	15.0	22.0	3.8
27 June 1997	1.5	1.1	1.0	1.1	-	-	-	-	-
7 Oct. 1998	4.7	4.6	300.0	10.4	2.0	2.5	17.0	91.8	17.6
20 Sept. 1999	3.7	2.8	19.2	2.0	1.7	2.0	6.4	10.4	3.0
12 Oct. 2000	3.3	2.3	55.6	3.2	1.2	1.6	35.0	110.6	1.6
11 May 2001	1.5	1.1	80.0	4.0	1.1	1.3	13.0	8.5	6.2
20 July 2001	2.0	1.4	20.9	2.1	1.6	1.6	4.7	15.0	4.5
4 May 2002	2.3	1.5	27.4	2.2	1.5	1.6	20.0	29.4	1.4
16 Nov. 2002	2.3	1.5	10.1	1.6	1.6	1.6	14.5	18.9	0.7
27 Nov. 2002	2.8	1.9	69.1	3.6	1.6	1.8	30.0	70.3	2.3
3 May 2003	1.0	1.0	1.0	1.1	-	-	-	-	-

[a]Q_p, peak discharge; RI_{Qp}, peak discharge return interval; BL, bed load volume (bulk measure); RI_{BL}, bed load volume return interval; Q_{cr1}, critical discharge for bed load entrainment; Q_{cr2}, end of bed load transport critical discharge; T_{BL}, duration of bed load transport; R_e, effective runoff (water runoff volume above the threshold discharge for bed load in the flood hydrograph); BL_R, mean bed load intensity (bulk measure).

best fitting distribution and its parameters were determined. Both Gumbel and lognormal distributions were found to fit reasonably (coefficient of Kolmorov-Smirnov $d = 0.106$ and $d = 0.156$, respectively, both indicating a nonsignificant difference). Recurrence intervals calculated by the two equations do not differ substantially (on average, ±6%) apart from the 14 September 1994 event, whose frequency of occurrence is predicted as 105 years according to the Gumbel distribution and as 53 years according to the lognormal. Bearing in mind the length of the available time series (17 years) and to avoid overestimating the weight of the September 1994 flood, return periods calculated through the lognormal distribution are chosen for subsequent comparisons.

[18] Return intervals of bed load volumes were also estimated considering the annual maximum volumes (bulk measure). Weibull and lognormal distributions were the best fitting ones (Figure 4b, coefficient of Kolmorov-Smirnov $d = 0.158$ and $d = 0.161$, respectively, both indicating a nonsignificant difference). Again, recurrence intervals do not differ substantially (on average, ±10%) applying the two distributions, apart for the September

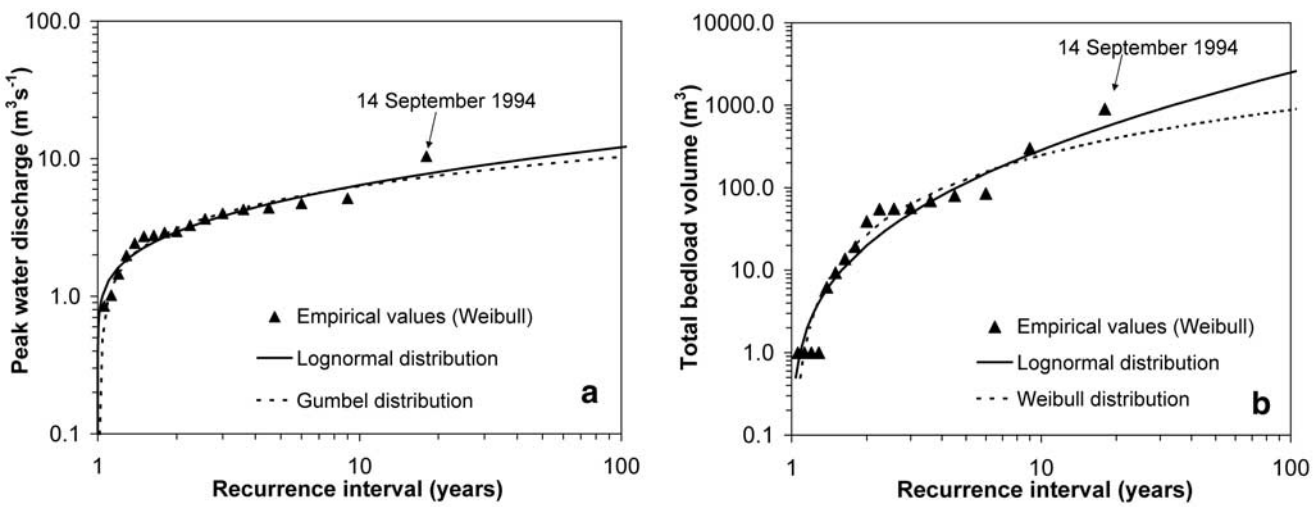

Figure 4. (a) Magnitude-frequency relationship for annual maximum peak discharge. Empirical values calculated by Weibull's plotting position ($i/N + 1$) are plotted with the curves of the lognormal and Gumbel distributions. (b) Magnitude-frequency relationship for annual maximum bed load volume. Empirical values calculated by Weibull's plotting position ($i/N + 1$) are plotted with the curves of the lognormal and Weibull distributions. The bed load volumes are expressed as bulk measure (including voids). See color version of this figure in the HTML.

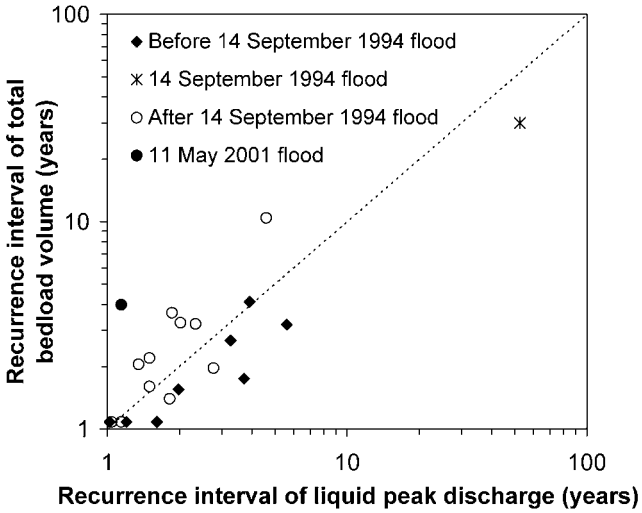

Figure 5. Comparison of recurrence intervals referring to liquid peak discharge and total bed load volumes for each recorded flood event. See color version of this figure in the HTML.

1994 event (105 years for Weibull and 30 years for lognormal). Similar to the peak water discharge analysis, the lognormal distribution is selected to calculate the frequency of occurrence of bed load volumes. Returns intervals of peak discharges and bed load volumes are reported for each of the 21 floods in Table 2.

[19] In Figure 5 a graphical comparison between return intervals for water discharge and bed load volumes of all the 21 flood events is shown. Most of post-1994 points fall above the equality line, whereas most pre-1994 data plot below it. The same result is evident even if return periods are calculated without the September 1994 data (graph not shown). Indeed, 1994 appears to represent a threshold for bed load transport in the Rio Cordon basin.

[20] On 14 September 1994, a flood presenting a peak water discharge of 10.4 m^3 s^{-1} and an hourly averaged bed load intensity of 225 m^3 h^{-1} (bulk measure) occurred. This event features a very short duration and a very high, infrequent peak flow rate (RI = 53 years), with a total bed load volume 900 m^3 (RI = 30 years). This low-frequency event, the largest recorded during the study period, also altered the stream geometry [*Lenzi*, 2001] and the sediment supply characteristics of the basin as a whole.

[21] After the 14 September 1994 flood event, a survey of sediment source areas was performed in order to identify reactivated and newly formed sediment sources. The area of reactivated sediment sources (77.8 m^2) exceeded that of the new ones (10.1 m^2). Slope instability was limited, but minor bank erosion and several bank failures were observed along the main stream and some tributaries. The main streambed appeared to have been the principal sediment source.

[22] An important new sediment source formed on 11 May 2001, simultaneous with a flood event in the main channel, during an intense snowmelt event without rainfall following a very snowy winter. Soil saturation mobilized a shallow landslide covering an area of 1905 m^2 which then turned into a mud flow moving along a small tributary (see Figures 3 and 6). A debris fan (volume ~4176 m^3) formed at the confluence with the Rio Cordon, thus feeding the main channel with medium and fine sediment.

Figure 6. Front view of the May 2001 mud flow fan delimitated by the Rio Cordon main channel. The rocky peaks in the background lie on the watershed divide. See color version of this figure in the HTML.

4. Frequency Analysis of Flood Events: Bed Load Partial Volumes and Transport Intensity

[23] Figure 7 shows a log-log plot of the relationship between annual maximum bed load volumes (in m^3) transported during 1, 4, 5, and 12 hour periods and their return period. For each year, maximum bed load volumes transported for each duration (i.e., continuous bed load period) were selected, treating them as independent values similar to what is commonly done for rainfall data. The lognormal distribution was found to be the best fitting one for durations up to 12 hours

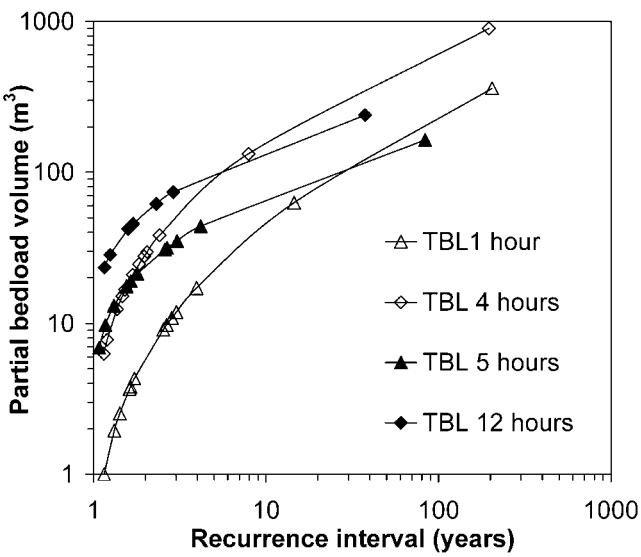

Figure 7. Recurrence interval of bed load partial volumes for different bed load durations. See color version of this figure in the HTML.

Table 3. Parameters Relative to Equation (1) for the Different Recurrence Intervals (RI)[a]

RI, years	a	n	R^2	p
2	8.40	0.72	0.93	<0.0005
3	17.43	0.56	0.85	<0.0005
4	26.35	0.47	0.76	<0.001
5	34.94	0.41	0.67	<0.005
10	72.71	0.25	0.34	<0.1
20	131.77	0.13	0.31	>0.1

[a]The correlation coefficient R^2 and the significance level p of the regression are also reported.

(nonsignificant p level of the Kolmogorov-Smirnov coefficient d). For longer bed load periods the sample size is too small to perform the fitting procedure. As for rainfall analysis, the monotonic trend is due to the incorporation of shorter duration into the longer ones, so that magnitudes increase with duration. The curves of bed load partial volume minus bed load duration relative to different return periods relation have a power form such that (for $T_{BL} < 12$ hours):

$$\mathrm{BL} = aT_{BL}^{n}, \tag{1}$$

where the parameters and correlation coefficient vary depending on the recurrence interval (Table 3). Figure 8a shows bed load intensity ($m^3\ h^{-1}$, obtained by dividing each bulk-measure partial volume by its duration) plotted versus bed load duration for return intervals from 2 to 20 years.

[24] A pronounced change occurs for bed load duration between 4 and 5 hours (Figures 7, 8a, and 8b). This change is determined by the bed load duration of the most important event as to sediment transport, the September 1994 event ($T_{BL} = 4$ hour). For frequent bed load events (RI close to 1) the longer the duration, the larger the yield (Figure 7). As the return interval increases, the period in which similar volumes are delivered decreases rapidly (for a 2-year recurrence interval a 4 hour event transports larger volumes than a 5 hour event). The shortest bed load periods, from 1 to 4 hours, exhibit very wide ranges in bed load transported volumes, as large as two orders of magnitude (1–360 m^3 for $T_{BL} = 1$ hour).

[25] This same evidence can be seen for bed load intensity (Figure 8a) where along with the expected general decrease of intensity for longer duration, the width of the variation band increases. There is a narrow range of intensity variation (between 4 and 8 $m^3\ h^{-1}$) for "ordinary" events (RI = 2 years) with durations from 1 to 12 hours. In contrast, short-duration (<4 hours), very infrequent events (RI = 20 years) have an intensity of almost 100 $m^3\ h^{-1}$, which is twice that recorded for longer (>4 hours) events of similar frequency (Figure 8a).

[26] In order to make the results about bed load intensity comparable to those from other basins a normalization is required. It was decided to render bed load intensity nondimensional by dividing it by the water discharge having the same return interval, calculated from the lognormal distribution. To have correct values of volumetric discharge ratios (Q_s/Q), bed load intensity in $m^3\ h^{-1}$ was first converted into $m^3\ s^{-1}$, and then porosity was eliminated (see section 3). As to the duration, a timescale is needed. It was decided to use the concentration time t_c given by equation (2) [*Ferro*, 2002], similar to the widely applied Kirpich's formula:

$$t_c = 0.00037\left(\frac{L}{\sqrt{S}}\right)^{0.8}, \tag{2}$$

where t_c is expressed in hours, L is the main channel length (in m), and S is the mean channel slope (in m m^{-1}) from the

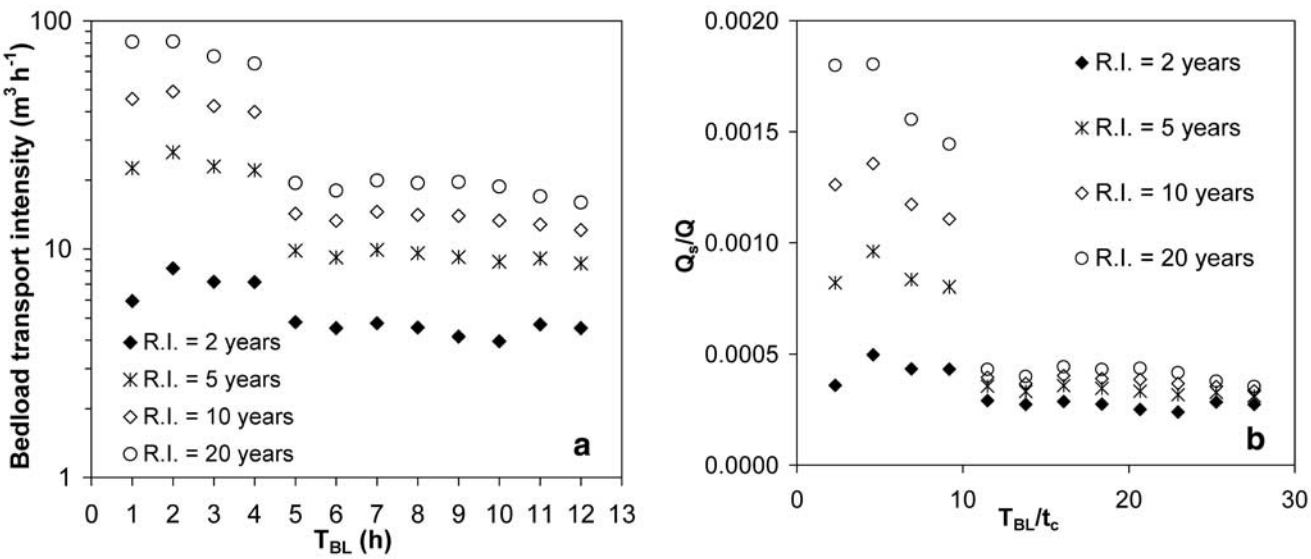

Figure 8. (a) Bed load hourly intensity (bulk measure) for different durations and recurrence interval. (b) Nondimensional bed load transport for different durations and recurrence interval. Q_s is the volumetric mineral bed load rate ($m^3\ s^{-1}$) normalized by the peak water discharge Q having the same return period, whereas T_{BL} is normalized by basin's concentration time t_c calculated by equation (2). See color version of this figure in the HTML.

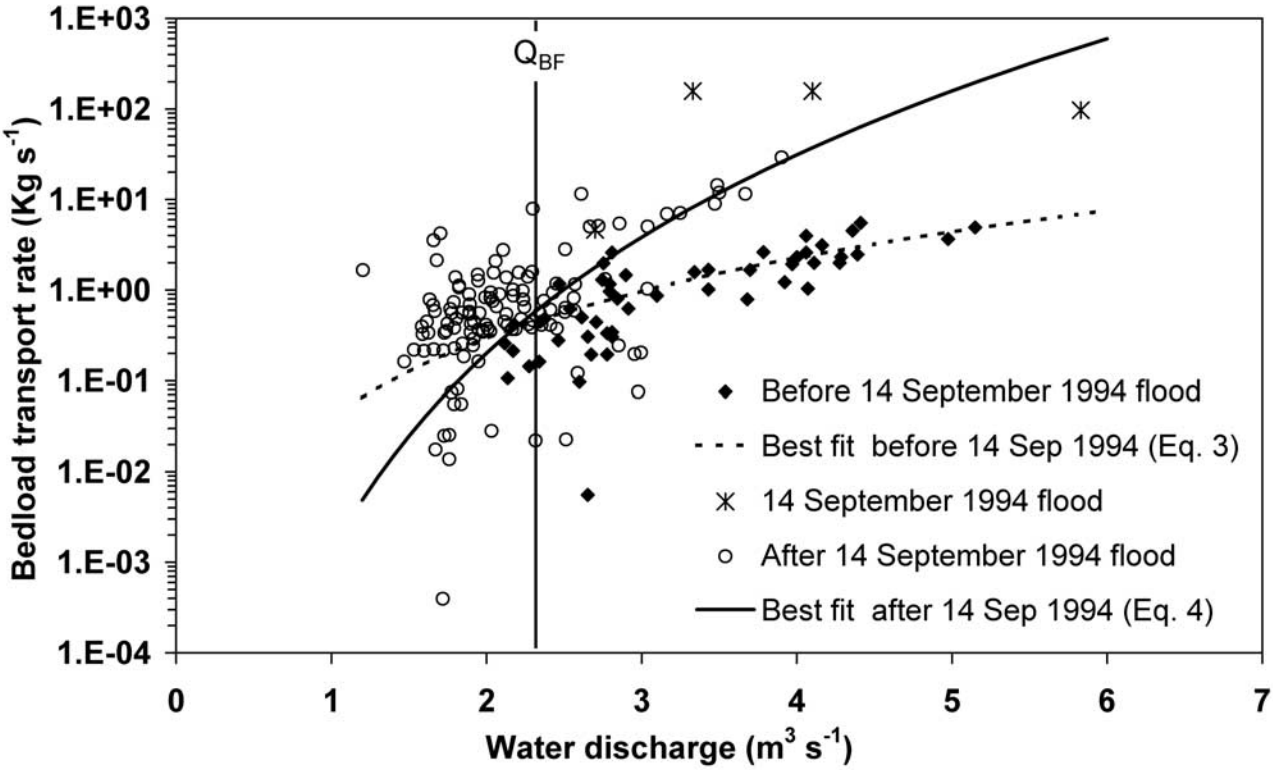

Figure 9. Semilog plot of measured pairs of bed load–flow rate, differentiated between pre-1994 and post-1994 events, and the 1994 flood. The bank-full discharge is also reported (vertical solid line). Regression curves (equations (3) and (4)) are also shown. Equation (4) does not include the 1994 points in the regression. See color version of this figure in the HTML.

basin divide to the station. For the Rio Cordon, with L = 2840 m and $S = 0.17$, the concentration time turns out equal to 0.435 hours. In Figure 8b the plot Q_s/Q versus T_{BL}/t_c is reported. In contrast to Figure 8a, this nondimensional graph features both axes in a linear scale, so that the slopes of the curves seem somewhat steeper. However, similar to Figure 8a, the larger the return period, the higher the step between short- and long-lasting bed load movements. The normalization through the concentration time results in a sharp decrease in bed load concentration associated with the 4-hour bed load duration occurring for $T_{BL}/t_c \sim 10$. After this nondimensional duration, the hourly averaged bed load concentration exhibits a reduced variability with its frequency of occurrence. For longer ratios an inversion among the different recurrence intervals' curves eventually happens, with a very narrow band of Q_s/Q values, on average ~0.01%. Instead, for $T_{BL}/t_c < 4$, nondimensional bed load intensity exhibits a much more relevant variability, ranging from 0.036 to almost 0.20%, i.e., ~6 times. This analysis, being based on hourly averaged data, neglects probable peaks of volumetric concentration that might be associated with the widely documented bed load pulses, and therefore Q_s/Q values are not that high even for very infrequent events.

5. Water Discharge–Bed Load Rate Relationship

[27] In order to seek possible different phases in bed load transport as those described in section 1 the coupling of the bed load rates (indicating a sediment flow in kg s^{-1}, in contrast to volumetric intensity in m^3 h^{-1}) and the associated water discharges were obtained following the procedure reported in section 2.2. Converting each volumetric (net of porosity) bed load value using the sediment specific weight 2650 kg m^{-3}, the relationship between hourly averaged rates is plotted in Figure 9.

[28] The data are grouped into three categories: September 1994 event (only four points), pre-1994 events, and post-1994 flood events. It is apparent that the former are displaced much higher than the others (up to 157 kg s^{-1}, i.e., 25 kg s^{-1} m^{-1}) in this semilog graph; in fact, the second highest intensity is only 30 kg s^{-1} (4.6 kg s^{-1} m^{-1}), and most points range from 0.1 to 3 kg s^{-1} (0.03–0.6 kg s^{-1} m^{-1}). A marked difference between pre-1994 and post-1994 floods is also clearly evident, the latter featuring larger bed load intensity for a similar water discharge. As already mentioned, the September 1994 flood represents a definite moment of change for the channel as to its morphology and sediment availability, and this point will be explored further in section 6. Extraordinarily high bed load rates of the September 1994 event might indicate that during this event a transport stage between a well-developed phase 2 and the beginning of phase 3 [*Warburton*, 1992] (see section 1) was reached. This hypothesis is supported by the findings of *Lenzi* [2004], who found in analyzing the particle displacements that near-equimobility conditions from pebbles to small boulders (32–256 mm, i.e., up to the D_{76} of the bed surface grain size distribution) were

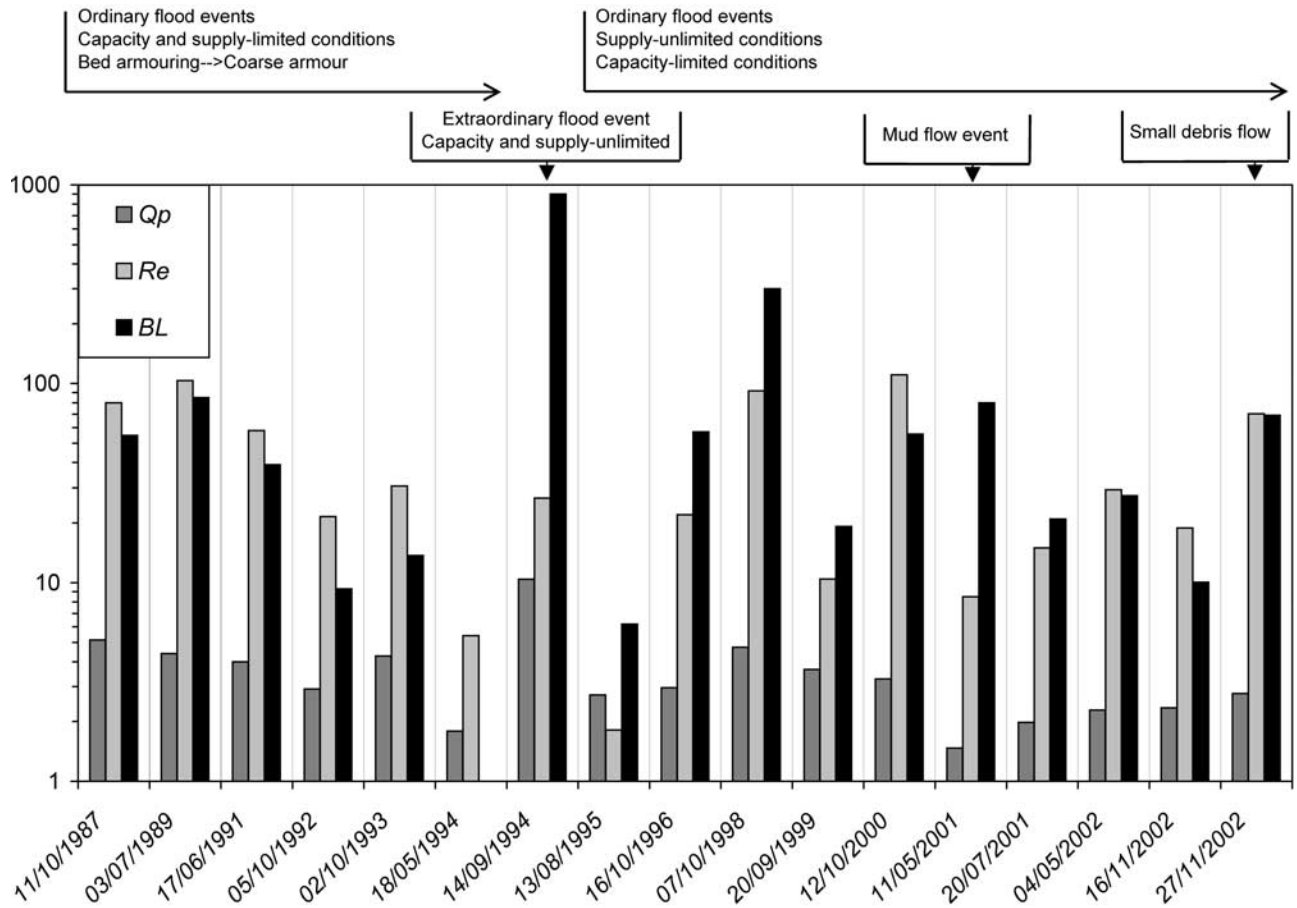

Figure 10. Main hydrological and sedimentological data of floods recorded in the Rio Cordon: Q_p, peak water discharge ($m^3\ s^{-1}$); R_e, effective runoff ($10^3\ m^3$); BL, bed load volume (m^3, bulk measure). See color version of this figure in the HTML.

established for the 1994 event ($Q_p = 10.4\ m^3\ s^{-1}$, RI around 50 years), while selective entrainment occurred for larger clast size (up to 512 mm). Sediment concentration during this flood reached a peak value of ~5–6%, with a 2% of fraction of coarse material [*D'Agostino and Lenzi*, 1999].

[29] As to the second largest event (the 1998 flood, $Q_p = 4.7\ m^3 s^{-1}$, RI ~5 years), *Lenzi* [2004] determined equimobility only for size classes up to the D_{40}. Therefore the vast majority of the points in Figure 9 should be connected to a transport phase 2, in the terms given by *Ashworth and Ferguson* [1989].

[30] Transport phase 1 (overpassing sand and fine gravel) is not considered here because Rio Cordon bed load data measured at the experimental station refer to diameter >20 mm only (see section 2). Also, given the steepness of the channel, a further possible shift toward hyperconcentrated flows and even debris flows may be envisaged for higher-magnitude events (RI > 100 years).

[31] Pre-1994 data apparently follow a power relationship ($N = 52$, $R^2 = 0.71$, $p < 0.05$):

$$Q_{s,kg} = 3.79 \times 10^{-2} Q^{2.954}, \quad (3)$$

where $Q_{s,kg}$ is the bed load discharge (in kg s^{-1}) and Q is the liquid discharge (in $m^3\ s^{-1}$). The presence of a breakpoint [*Ryan et al.*, 2002] was sought using piecewise regression but with no success.

[32] As to post-1994 points, a more complex pattern is featured. The scatter is substantially larger and for water discharges below 3 $m^3\ s^{-1}$, two or maybe more trends are present, each showing much different bed load rates, ranging over two orders of magnitude (Figure 9). Again, the piecewise regression did not lead to any reliable results, and the best fit equation reads as follows ($N = 124$, $R^2 = 0.77$, but with a lower significance being $p = 0.10$):

$$Q_{s,kg} = 1.29 \times 10^{-3} Q^{7.280}. \quad (4)$$

[33] Two aspects can be pointed out in comparison to the pre-1994 data: the overall higher bed load rates during post-1994 events for similar liquid discharges and their much steeper curve for flow rates between 3 and 4 $m^3\ s^{-1}$ where they display a single, poorly represented relationship. As to the former point, bed load rates around an approximate bank-full value of 2.3 $m^3\ s^{-1}$ equals 0.43 kg s^{-1} (0.08 kg $s^{-1}\ m^{-1}$) for pre-94 period (using equation (3)), while it turns out (applying equation (4)) to be 0.55 kg s^{-1} (0.09 kg $s^{-1}\ m^{-1}$) for the post-94 events.

[34] The reason for these differences likely rests on the abrupt increase in the availability of relatively fine (still

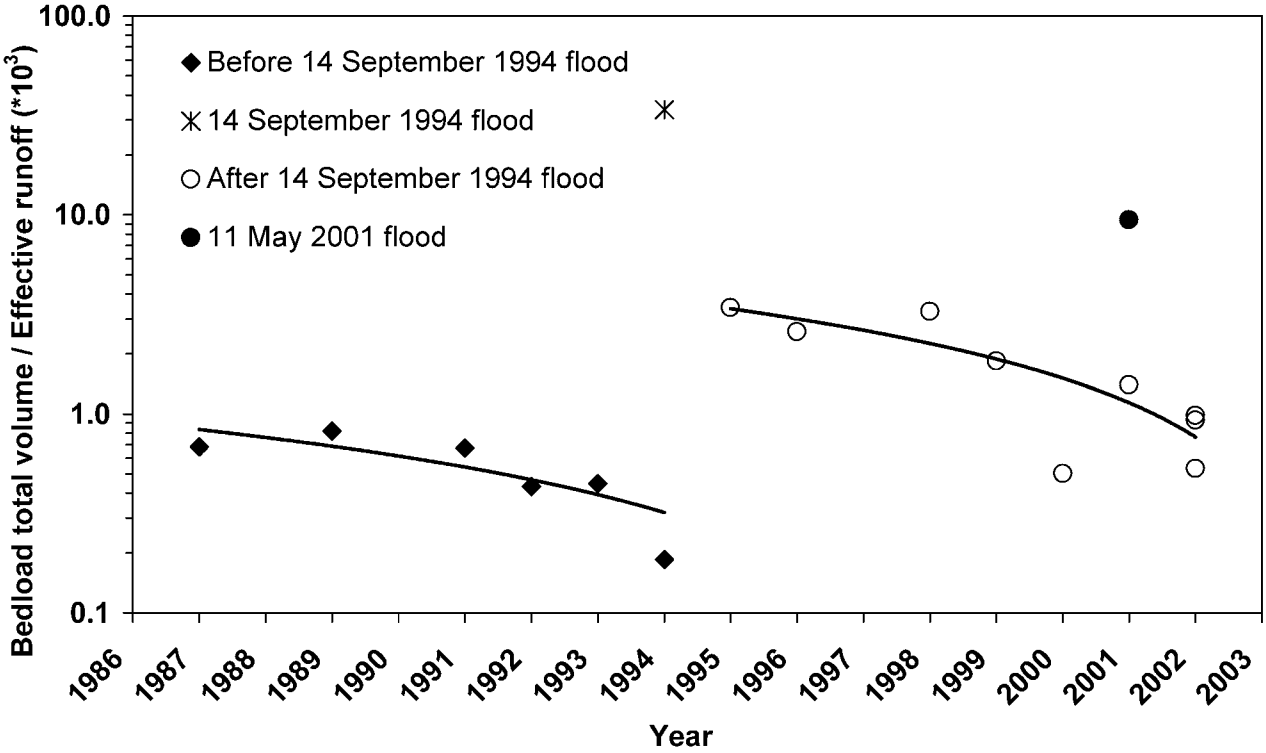

Figure 11. The ratio bed load volume/effective runoff ($\times 10^3$) over 17 years of recording. Solid lines represent the best fit curves for the two periods (pre-1994 and post-1994), excluding the 1994 and 2001 events. Bed load volume is expressed as bulk measure. See color version of this figure in the HTML.

>20 mm) and more mobile sediment due to the breaking up of the bed armor during the September 1994 event. In addition, the concomitant changes that altered the previous step pool morphology, i.e., the reduction of the steepness factor *c* [*Lenzi*, 2001], may have led to a channel configuration where less energy is dissipated by spill resistance associated with steps, thus increasing the sediment transport efficiency of a given water discharge. As to the scatter within post-1994 data, this probably is caused by a progressive reduction with time of sediment availability. From the results described so far it becomes dramatically evident that an analysis performed using hydraulic variables only is far from being exhaustive and that the temporal evolution of the system deserves a closer look.

6. Temporal Trends in the Bed Load Transport

[35] The hydrological and sedimentological data of floods recorded in the Rio Cordon between 1987 and 2002 are presented chronologically in Figure 10, where limited and unlimited sediments supply periods are highlighted, separated by the September 1994 event. During this extreme event the channel bed was the main source of sediment for bed load transport [*Lenzi et al.*, 2003] mostly because such a large discharge was able to destroy the streambed armor layer formed over the years. Also, during the September 1994 flood, old sediment sources were reactivated and new ones were created. Fine- and medium-size sediments eroded from the hillslopes were stored in the stream network as the flood waned and were subsequently removed and transported downstream by ordinary floods in 1996, 1998, and 2000.

[36] Analogously, quasi-unlimited sediment supply conditions occurred in the Rio Cordon as a consequence of the 2001 mud flow. Besides the May 2001 event's high bed load transport the availability of sediments from the newly formed fan likely allowed the small July 2001 flood to mobilize 21 m^3 of bed load material. The three floods in 2002 show high sediment loads too, and this may be partly an inheritance of the May 2001 mud flow, even though a small debris flow (Figure 3) that occurred close to the measuring station during the November 2002 event might have contributed considerably to this flood's high bed load transport.

[37] The effective runoff R_e, determined for each flood as the hydrograph volume exceeding the detected threshold discharges ($Q_{cr1\text{-}2}$) from the beginning to the end of the bed load transport, provides a means to normalize total bed load volumes (BL) and thus allows us to infer temporal trends in the bed load yields. Figure 11 shows a semilogarithmic plot of the ratio BL/R_e (with $R_e$expressed as 10^3 m^3) for each flood. The BL/R_e ratio exhibits two decreasing trends over the 1986–1993 and 1995–2002 periods, and its value for the September 1994 flood is >1 order of magnitude larger than in the other floods, except for the May 2001 event. Before 1994, the ratio was always below 1, whereas afterward, it is mostly above 1, as a response to such a destabilizing event. The decreasing trends can be ascribed to the flushing of sediment from the streambed and other active sources by "ordinary" events. However, the trend line shown for the post-1994 events might not be entirely significant because of the sediment supplying effect of the May 2001 event which may have "raised" the ratios thereafter, but the

scarcity of points prevents any definitive assertion. When the bed structure is disrupted by very large flow rates (e.g., September 1994) or the channel is fed with easily transportable sediment (e.g., May 2001), the bed load volumes can be >1 order of magnitude larger. The analysis of bed load production through the effective runoff confirms in a dimensionless manner what was already envisaged in section 5 about the role of sediment supply derived from the September 1994 extreme event and from the May 2001 mud flow.

7. Conclusions

[38] This paper has presented the results from a combined frequency analysis of peak water discharges and bed load final and partial volumes on the basis of a long (17 year) time series of field data from a high-gradient stream of the Alps. The large variability in bed load final volumes and hourly transport rates emphasizes the basic role played by in-channel sediment availability and by the degree of coupling between the channel and hillslope processes such as debris and mud flows, which occurred twice during the study period. The highest bed load rates measured in the Rio Cordon (up to 157 kg s^{-1}, i.e., 25 kg $s^{-1}m^{-1}$) are very large compared to values found in the literature on mountain streams; this is probably because previous studies evaluated bed load rates during snowmelt events or, at most, flow rates not more than twice the bank-full discharge. In the Rio Cordon, instead, a low-recurrence event having a peak discharge around 4 times bank-full demonstrates that very high bed load rates can be reached in such steep channels.

Notation

BL	bed load volume (bulk measure), m^3.
BL_R	mean bed load intensity (bulk measure), m^3 h^{-1}.
c	step pool relative steepness factor, equal to $(H/L_s)/S$.
D_x	xth percentile of the grain size distribution, mm.
D_m	mean diameter of the grain size distribution, mm.
H	step height, m.
L	length of the main channel, m.
L_s	step spacing, m.
N	data set size.
p	significance level.
Q	water discharge, m^3 s^{-1}.
Q_{BF}	water discharge at bank-full stage, m^3 s^{-1}.
Q_{cr1}	critical discharge for the initiation of bed load motion, m^3 s^{-1}.
Q_{cr2}	critical discharge corresponding to the end of bed load motion, m^3 s^{-1}.
Q_p	peak water discharge, m^3 s^{-1}.
Q_s	bed load discharge by volume (net of porosity), m^3 s^{-1}.
$Q_{s,kg}$	bed load discharge by weight, kg s^{-1}.
R_e	effective runoff, m^3.
RI	recurrence interval, years.
S	mean longitudinal slope of the channel, from the divide to the station, m m^{-1}.
T_{BL}	duration of bed load motion, hours.
t_c	concentration time of the basin, hours.

[39] **Acknowledgments.** The ARPAV center of Belluno, the Avalanche Center of Arabba (Veneto Region), and particularly, A. Lucchetta, G. R. Scussel, and F. Sommavilla are kindly acknowledged for providing the Rio Cordon data. We are grateful to T. Corso and W. Testor for their assistance and field work. This research was funded by the University of Padua, project "Valutazione della pericolosità connessa a colate detritiche sui conoidi Alpini" directed by M. Lenzi, by the EU project PL510739 "Epic force" (evidence-based policy for integrated control of forested river catchments in extreme rainfall and snowmelt), by the Italian Minister "MIUR ex 60%," and in the framework of the U.S. NSF project for Western Europe "Flow hydraulics along step pool channels," coordinated by E. E. Wohl (Colorado State University). Finally, the two anonymous reviewers are kindly acknowledged for their valuable suggestions and corrections, which greatly improved the paper.

References

Andrews, E. D. (1984), Bed-material entrainment and hydraulic geometry of gravel-bed rivers in Colorado, *Geol. Soc. Am. Bull.*, *5*, 371–378.

Andrews, E. D., and J. M. Nankervis (1995), Effective discharge and the design of channel maintenance flows for gravel-bed rivers, in *Natural and Anthropogenic Influences in Fluvial Geomorphology: The Wolman Volume*, *Geophys. Monogr. Ser.*, vol. 89, edited by J. E. Costa et al., pp. 151–164, AGU, Washington, D. C.

Andrews, E. D., and J. D. Smith (1992), A theoretical model for calculating marginal bedload transport rates of gravel, in *Dynamics of Gravel-Bed Rivers*, edited by P. Billi et al., pp. 41–48, John Wiley, Hoboken, N. J.

Ashworth, P. J., and R. I. Ferguson (1989), Size-selective entrainment of bed load in gravel bed streams, *Water Resour. Res.*, *25*(4), 627–634.

Asti, G. (1999), La valutazione del trasporto solido nel bacino sperimentale del Rio Cordon, M.S. thesis, Univ. of Padua, Padua, Italy.

Bathurst, J. C., W. H. Graf, and H. H. Cao (1987), Bedload discharge equations for steep mountain rivers, in *Sediment Transport in Gravel-Bed Rivers*, edited by C. R. Thorne, J. C. Bathurst, and R. D. Hey, pp. 453–491, John Wiley, Hoboken, N. J.

Billi, P., V. D'Agostino, M. A. Lenzi, and L. Marchi (1998), Bedload, slope and channel processes in a high altitude Alpine torrent, in *Gravel-Bed Rivers in the Environment*, edited by P. C. Klingeman et al., pp. 15–38, Water Resour. Publ., Highlands Ranch, Colo.

Blizard, C. R. (1994), Hydraulic variables and bedload transport in East St. Louis Creek, Rocky Mountains, Colorado, M.S. thesis, Colo. State Univ., Fort Collins.

Bogen, J. (1995), Sediment transport and deposition in mountain rivers, in *Sediment and Water Quality in River Catchments*, edited by I. Foster, A. Gurnell, and B. Webb, pp. 437–451, John Wiley, Hoboken, N. J.

Carling, P. A. (1988), The concept of dominant discharge applied to two gravel-bed streams in relation to channel stability thresholds, *Earth Surf. Processes Landforms*, *13*, 355–367.

D'Agostino, V., and M. A. Lenzi (1999), Bedload transport in the instrumented catchment of the Rio Cordon: Part II. Analysis of the bedload rate, *Catena*, *36*(3), 191–204.

D'Agostino, V., M. A. Lenzi, and L. Marchi (1994), Sediment transport and water discharge during high flows in an instrumented watershed, in *Dynamics and Geomorphology of Mountain Rivers*, *Lect. Notes Earth Sci.*, vol. 52, edited by P. Ergenzinger and K. H. Schmidt, pp. 67–81, Springer-Verlag, New York.

Dalla Fontana, G., and L. Marchi (1998), GIS indicators for sediment sources study in Alpine basins, in *Hydrology, Water Resources and Ecology in Headwaters*, edited by K. Kovar, U. Tappeiner, N. E. Peters, and R. G. Carig, *IAHS Publ.*, *248*, 553–560.

Dalla Fontana, G., and L. Marchi (2003), Slope-area relationships and sediment dynamics in two alpine streams, *Hydrol. Processes*, *17*, 73–87.

Fattorelli, S., H. M. Keller, M. A. Lenzi, and L. Marchi (1988), An experimental station for the automatic recording of water and sediment discharge in a small alpine watershed, *Hydrol. Sci. J.*, *33*(6), 607–617.

Ferro, V. (2002), *La sistemazione dei bacini idrografici*, McGraw-Hill, New York.

Jackson, W. L., and R. L. Beschta (1982), A model of two-phase bedload transport in an Oregon Coast Range stream, *Earth Surf. Processes Landforms*, *7*, 517–527.

Johnejack, K. R., and W. F. Megahan (1991), Sediment transport in headwater channels in Idaho, in *Fifth Interagency Sedimentation Conference, Las Vegas, NV*, edited by S.-S. Fan and Y.-H. Kuo, pp. 4-155–4-161, Fed. Energy Regul. Comm., Washington, D. C.

Knighton, A. D. (1998), *Fluvial Forms and Processes: A New Perspective*, Edward Arnold, London.

Lenzi, M. A. (2001), Step-pool evolution in the Rio Cordon, northeastern Italy, *Earth Surf. Processes Landforms*, *26*, 991–1008.

Lenzi, M. A. (2004), Displacement and transport of marked pebbles, cobbles and boulders during floods in a steep mountain stream, *Hydrol. Processes*, *18*, doi:10.1002/hyp.1456.

Lenzi, M. A., and L. Marchi (2000), Suspended sediment load during floods in a small stream of the Dolomites (northeastern Italy), *Catena*, *39*, 267–282.

Lenzi, M. A., V. D'Agostino, and P. Billi (1999), Bedload transport in the instrumented catchment of the Rio Cordon: Part I. Analysis of bedload records, conditions and threshold of bedload entrainment, *Catena*, *36*(3), 171–190.

Lenzi, M. A., L. Mao, and F. Comiti (2003), Interannual variation of sediment yield in an alpine catchment, *Hydrol. Sci. J.*, *48*(6), 899–915.

Lisle, T. E. (1995), Particle size variations between bed load and bed material in natural gravel bed channels, *Water Resour. Res.*, *31*(4), 1107–1118.

Meyer-Peter, E., and R. Muller (1948), Formulas for bedload transport, paper presented at 2nd Meeting of International Association for Hydraulic Structures Research, Stockholm, Sweden.

Mizuyama, T. (1977), Bedload transport in steep channels, Ph.D. thesis, Kyoto Univ., Kyoto, Japan.

Montgomery, R. D., and J. M. Buffington (1997), Channel-reach morphology in mountain drainage basin, *Geol. Soc. Am. Bull.*, *109*(5), 596–611.

Parker, G., P. C. Klingeman, and D. G. McLean (1982), Bedload size and distribution in paved gravel-bed stream, *J. Hydraul. Div. Am. Soc. Civ. Eng.*, *108*(HY4), 544–571.

Rickenmann, D. (1990), Bedload transport load capacity of slurry flows at steeps slopes, *Mitt. Versuchsanst. Wasserbau, Hydrol. Glaziol. 103*, Eidg. Tech. Hochsch.-Zurich, Zurich, Switzerland.

Rickenmann, D. (1994), Bedload transport and discharge in the Erlenbach stream, in *Dynamics and Geomorphology of Mountain Rivers*, *Lect. Notes Earth Sci.*, vol. 52, edited by P. Ergenzinger and K. H. Schmidt, pp. 53–66, Springer-Verlag, New York.

Rickenmann, D. (1997), Sediment transport of Swiss torrents, *Earth Surf. Processes Landforms*, *22*, 937–951.

Rickenmann, D. (2001), Comparison of bedload transport in torrents and gravel bed streams, *Water Resour. Res.*, *37*(12), 3295–3305.

Rickenmann, D., V. D'Agostino, G. Dalla Fontana, M. A. Lenzi, and L. Marchi (1998), New results from sediment transport measurements in two Alpine torrents, in *Hydrology, Water Resources and Ecology in Headwaters*, edited by K. Kovar et al., *IAHS Publ.*, *248*, 283–289.

Ryan, S. E., L. S. Porth, and C. A. Troendle (2002), Defining phases of bedload transport using piecewise regression, *Earth Surf. Processes Landforms*, *27*, 971–990.

Smart, J. M. (1984), Sediment transport formula for steep channels, *J. Hydraul. Eng.*, *110*(3), 267–276.

Smart, J. M., and M. N. R. Jaeggi (1983), Sediment transport on steep slopes, *Mit. Versuchsanst. Wasserbau, Hydrol. Glaziol. 64*, Eidg. Tech. Hochsch.-Zurich, Zurich, Switzerland.

StatSoft (2002), STATISTICA, version 6, Tulsa, Okla.

Suszka, L. (1991), Modification of transport rate formula for steep channels, in *Fluvial Hydraulics of Mountain Regions*, edited by A. Armani and G. G. Silvio, pp. 59–70, Springer-Verlag, New York.

Warburton, J. (1992), Observations of bed-load transport and channel bed changes in a proglacial mountain stream, *Arct. Alpine Res.*, *24*(3), 195–203.

Wilcock, P. R., and B. W. McArdell (1993), Surface-based fractional transport rates: Mobilization thresholds and partial transport of sand-gravel sediment, *Water Resour. Res.*, *29*(4), 1297–1312.

Wohl, E. E. (2000), *Mountain Rivers*, *Water Resour. Monogr. Ser.*, vol. 14, AGU, Washington, D. C.

F. Comiti, M. A. Lenzi, and L. Mao, Department of Land and Agroforest Environments, University of Padova, Agripolis, viale dell'Università 16, 35020 Legnaro (Padova), Italy. (francesco.comiti@unipd.it; marioaristide.lenzi@unipd.it; luca.mao@unipd.it)